International Journal of Steel Structures 17(3): 1087-1102 (2017)
DOI 10.1007/s13296-017-9018-5
ISSN 1598-2351 (Print)
ISSN 2093-6311 (Online)

International Journal of
STEEL
STRUCTURES
www.springer.com/journal/13296

An Efficient Formulation for Thin-walled Beams Curved in Plan

Ashkan Afnani[1,*], R. Emre Erkmen[2], and Vida Niki[1]

[1]*Graduate Research Assistant, School of Civil and Environmental Engineering, University of Technology, Sydney, NSW 2007, Australia*
[2]*Lecturer, School of Civil and Environmental Engineering, University of Technology, Sydney, NSW 2007, Australia*

Abstract

An efficient formulation is developed for the elastic analysis of thin-walled beams curved in plan. Using a second-order rotation tensor, the strain values of the deformed configuration are calculated in terms of the displacement values and the initial curvature by adopting the right extensional strain measure. The principle of virtual work is then used to obtain the nonlinear equilibrium equations, based on which a finite element beam formulation is developed. The accuracy of the method is confirmed through comparison with test results, shell finite element formulations and other curved beam formulations from the literature. It is also shown that the results of the developed formulation are very accurate for the cases where initial curvature is large.

Keywords: thin-walled, curved in plan, finite element, large initial curvature

1. Introduction

Curved members are extensively used in engineering structures such as highway interchanges and railway bridges. A horizontally curved member subjected to a vertical out-of-plane loading undergoes torsion, compression, and biaxial moments as primary actions. Apart from that, second order bending moments and torsional moments are generated by coupling between the angle of twist and the bending moment and between the vertical displacement and the torsional moment, respectively. Traditionally, horizontally-curved beams were numerically analysed by a sequence of short straight beam elements. However, it was shown (Sawko, 1967) that the straight idealisation error may be significant even for small included angle (in the order of 1°). Consequently, several researchers proposed curved beam finite elements, starting from the late 1960s. Sawko (1967), Brookhart (1967) and Young (1969) proposed finite element models for beams curved in plan. El-Amin & Brotton (1976) included the warping restraint in the formulation of a displacement-based finite element. Later, El-Amin & Kasem (1978) improved the efficiency of the model by assigning higher order polynomials for the angle of twist.

Received May 15, 2016; accepted January 29, 2017;
published online September 30, 2017

*Corresponding author
Tel: +61-2-9514-9769, Fax: +61-2-9514-2633
E-mail: ashkan.afnaniesfandabadi@student.uts.edu.au

Akhtar (1987) obtained the stiffness matrix of a circular member using a flexibility matrix. Krenk (1994) derived the stiffness matrix for beam element by using the static equilibrium state along with the principle of stationary complementary energy. However, neither of the two finite elements discussed herein is applicable to a horizontally curved beam because the torsional actions are not considered in formulating the stiffness matrices. Therefore, these two methods can be used when the curvature of the beam is in the vertical plane as in arches.

All the aforementioned numerical models were based on the linear analysis of curved beams. However, the effect of geometric nonlinearity may be significant for curved members even under serviceability stage and therefore, several finite element formulations have been developed to capture the geometrically nonlinear behaviour. These works include those of Fukumoto & Nishida (1981) and Yoshida & Maegawa (1983) for the analysis of horizontally curved I-beams. Iura & Atluri (1988) developed a three dimensional beam element for elements curved in space. Richard Liew *et al*. (1995) used triangular and quadrilateral shell elements in the finite element program ABAQUS to study the second-order behaviour of horizontally curved I-beams by focusing on the effect of radius of curvature to span length and the residual stresses on the ultimate load capacity of the member. Based on the study, they proposed a design formula for predicting the ultimate load-carrying capacity of horizontally curved I-beams.

All the nonlinear studies discussed so far (Fukumoto & Nishida, 1981; Richard Liew *et al*., 1995; Yoshida &

Maegawa, 1983) are limited to beams with very small horizontal curvature. Yoo *et al*. (1996) presented a finite element formulation by the principle of minimum potential energy. They included the effect of curvature in derivation of elastic and geometric stiffness matrices; therefore, the model was capable of analysing beams with higher initial curvature.

Several researchers have worked on developing finite elements based on the "geometrically exact beam theory". The motivation is that in developing the finite elements based on energy equations, strain-displacement relations are used to specify the strain based on the kinematic assumptions that relate the displacement at an arbitrary point on the cross-section to the displacement and rotations of the centre line. In order to separate the linear relations from the nonlinear part, approximations are normally made. However, it has been reported (Crisfield, 1990; Simo & Vu-Quoc, 1987) that this sort of approximation may result in the loss of some important terms in the strain-displacement relations, resulting in overly stiff nonlinear response. To solve the problem, the geometrically exact formulations have been proposed that are based on the resultants of the equilibrium equations. Simo (1985) developed the first finite element formulations based on the geometrically exact descriptions, without considering warping effects. Simo & Vu-Quoc (1991) added the torsional warping effect and the warping due to combined bending and torsion to the theory. Sandhu *et al*. (1990) and Crisfield (1990) developed a co-rotational formulation for curved beams undergoing large deformations. Pi & Trahair (1997) studied the behaviour of horizontally curved beams under vertical loading and developed a curved finite element. They concluded that when the included curvature in the beam is small, the nonlinear behaviour of the beam becomes similar to straight beams (i.e. lateral-torsional buckling becomes the dominant mode of failure). However, when the included angle is relatively large, the coupling between the bending moment and the twisting moment becomes significant, and the nonlinear behaviour starts far before the lateral-torsional buckling load. Pi *et al*. (2005) stated that inclusion of Wagner moments and Wagner terms considerably increases the accuracy of the models dealing with cases with large torsional actions. Erkmen & Bradford (2009) extended the work of Pi & Trahair (1997) the by developing a finite element formulation for the elastic dynamic analysis of horizontally curved I-beams. It was observed by the authors that the response of curved beams is considerably different when the initial curvature is medium to large. However, the formulation based on Pi & Trahair (1997) is accurate when the initial curvature per the beam element is relatively small.

In this study, the right extensional strain definition is adopted to develop a curved beam formulation. Using a second-order rotation tensor, the curvature values of the deformed configuration are calculated in terms of the displacement values and the initial curvature. The principle of virtual work is then used to obtain the nonlinear equilibrium equations, based on which, a finite element beam formulation is developed.

The outline of this paper can be summarised as follows. In Section 2, the kinematics of the curved beam and the adopted rotation matrix are presented, followed by the calculation of the curvature values of the deformed configuration. The Stresses and cross-sectional stress resultants are defined in Section 3 followed by the loading conditions in Section 4. Principal of virtual work is used in Section 5 to obtain the nonlinear equilibrium equations, which are linearized to obtain the corresponding finite element formulation. In Section 6, numerical examples are performed. The accuracy of the proposed model is verified through comparisons with test results from literature and numerical results obtained from a full shell-type finite element modelling of the curved beam. Section 7 provides a summary and conclusions for this study. Further details of the derivation of the formulation are presented in Appendices A to E.

2. Kinematics of the Problem

2.1. Basic assumptions

A schematic of a curved beam can be seen in Fig. 1, where the undeformed and deformed configurations of the curved beam are shown by dashed and solid lines, respectively.

Formulation of the beam element is based on the following assumptions:

- The current formulation is limited to beams that are initially curved in a single plane.
- Since a beam formulation is developed, the cross-section is assumed to remain rigid throughout the deformation.
- The shear strains are considered to be negligible on the mid-surface in line with Vlasov kinematics.
- Strains are assumed small and under the elastic range, however the rotations and deflections are kept up to the second order, and thus assumed moderate.

There are alternative strain and conjugate stress measures in finite elasticity. In order to accurately relate the stresses and strains, constitutive relations based on hyper-elasticity have to be adopted. However, in case of small strains that we assume, these relations can reduce to Hook's law. On the other hand, under this assumption, keeping the second order terms according to different strain measures makes difference in the results. In this paper, in line with de Veubeke (1972), Pai & Palazotto (1995) and Pai *et al*. (1998), we adopt Hook's constitutive relation along with the right extensional strain up to the second-order terms. The comparison of the developed curved beam formulation based on right extensional strain of the polar decomposition with finite element shell solutions and test results verifies the accuracy.

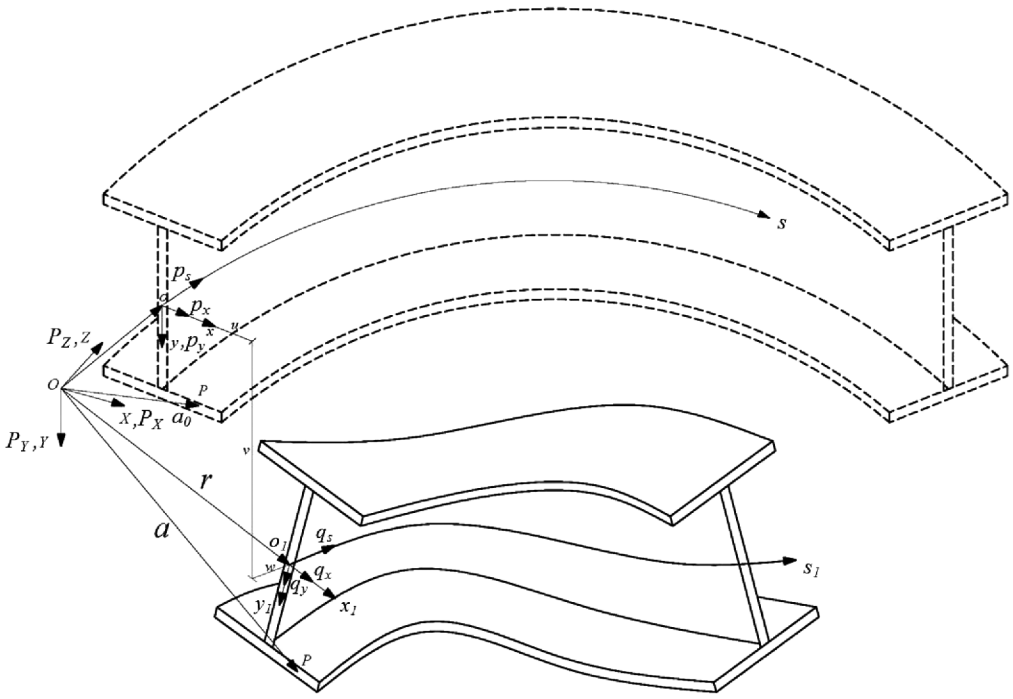

Figure 1. Schematic of the curved beam: Coordinate systems and displacements.

2.2. Displacements

In order to incorporate large deformations of the curved beam, we assign a fixed space and two sets of coordinate systems for undeformed and deformed configurations of the body. The fixed space axes *OXYZ* are formed by the orthogonal basis provided by the triad $\mathbf{P}(\mathbf{P}_X, \mathbf{P}_Y, \mathbf{P}_Z)$. In order to demonstrate the undeformed configuration of the curved beam, a body-attached *oxys* coordinate system is adopted, the origin of which is placed at the centroid of the cross-section. The axis *os* is tangent to the axis of the beam, while the axes *ox* and *oy* lie in the plane of the cross-section and pass through the principal axes. The three components of the triad $\mathbf{p}(\mathbf{p}_x, \mathbf{p}_y, \mathbf{p}_z)$ form an orthogonal basis of the system *oxys* in the direction of the tangent of the axes *ox*, *oy* and *os* respectively as depicted in Fig. 1. The deformed configuration of the curved beam is shown by another set of axes $o_1x_1y_1s_1$, which form a (Lagrangian) curvilinear coordinate system that changes with the deformation of the member and coincides with *oxys* in the undeformed state. Similar to the undeformed coordinate system, the axis o_1s_1 lies in the direction tangent to the axis of the deformed beam and the axes o_1x_1 and o_1y_1 lie in the cross-sectional plane of the deformed configuration. A triad $\mathbf{q}(\mathbf{q}_x, \mathbf{q}_y, \mathbf{q}_z)$ forms the orthogonal basis for the latter system, the components of which are in the tangent direction of o_1x_1, o_1y_1 and o_1s_1 respectively.

Based on the above definition, the position vectors of a point *P* on the cross-section before and after the deformation can be stated as

$$\begin{aligned} \mathbf{a}_0 &= \mathbf{r}_0 + x\mathbf{p}_x + y\mathbf{p}_y \\ \mathbf{a} &= \mathbf{r} + x\mathbf{q}_x + y\mathbf{q}_y - \bar{\omega}(x, y)p(s)\mathbf{q}_s \end{aligned} \tag{1}$$

where $\mathbf{r}_0$ and $\mathbf{r}$ are the position vectors of the centroid *o* before and after the deformation respectively in the fixed axes *OXYZ*, $\bar{\omega}(x, y)$ is the normalized section warping displacement function and $p(s)$ is the warping amplitude. The position vector of the deformed centroid can be obtained from the undeformed centroid and the displacement components as (Fig. 1)

$$\mathbf{r} = \mathbf{r}_0 + u\mathbf{p}_x + v\mathbf{p}_y + w\mathbf{p}_s \tag{2}$$

The orientation of the triad $\mathbf{q}$ is determined by the use of a rotation tensor $\mathbf{R}$ multiplied by the triad $\mathbf{p}$ as

$$\mathbf{q} = \mathbf{R}\mathbf{p} \tag{3}$$

According to the orthogonality condition of the rotation tensor, i.e. $\mathbf{R}^T\mathbf{R}=\mathbf{I}$, only six out of the nine components of the rotation tensor are linearly independent. According to the Euler-Rodriguez formula (Koiter 1984), the rotation tensor can be calculated in terms of the rotation components ϕ_1, ϕ_2 and ϕ_3 around the axes *OX*, *OY* and *OZ*, respectively, as

$$R_{ij} = \delta_{ij}\left(1 - \tfrac{1}{2}\phi_k\phi_k\right) + \varepsilon_{ikj}\phi_k + \tfrac{1}{2}\phi_i\phi_j + o\left(|\phi|^3\right) \tag{4}$$

where δ_{ij} is the Kronecker delta, ε_{ikj} is the permutation symbol and $o(|\phi|^3)$ refers to terms higher than second order. The indices 1, 2 and 3 indicate the *x*, *y* and *s* axes,

respectively. According to the right hand rule sign convention, the rotation components ϕ_i are related to the derivatives of the displacement of the beam centroid as

$$\phi_X = -v' \qquad \phi_Y = \tilde{u}' \tag{5}$$

For a beam curved in plan, $\tilde{u} = u' + \kappa_0 w$ where u, v and w are displacement components along x, y and s directions respectively, and κ_0 is the initial curvature of the curved beam's centroidal locus about the Y axis . By neglecting rotation terms higher that the second order, the rotation matrix can be written as

$$\mathbf{R} = \begin{bmatrix} 1-\frac{1}{2}\left(\phi^2+\tilde{u}'^2\right) & -\phi-\frac{1}{2}\tilde{u}'v' & \tilde{u}'-\frac{1}{2}\phi v' \\ \phi-\frac{1}{2}\tilde{u}'v' & 1-\frac{1}{2}\left(\phi^2+v'^2\right) & v'+\frac{1}{2}\phi\tilde{u}' \\ -\tilde{u}'-\frac{1}{2}\phi v' & -v'+\frac{1}{2}\phi\tilde{u}' & 1-\frac{1}{2}\left(\tilde{u}'^2+v'^2\right) \end{bmatrix} \tag{6}$$

in which f is the twist rotation of the cross-section, and the symbol ( )' denotes the derivative with respect to the S coordinate.

2.3. Curvature values at deformed configuration

In the deformed configuration, the curvatures in x and y directions, i.e. k_x and k_y, and the twist can be obtained by Frenet-Serret formulae (Love, 1944) using the afore-mentioned rotation matrix (Appendix A) to be

$$\kappa_x = (1+\varepsilon)^{-1}\left[-v'' - \tfrac{1}{2}\tilde{u}'\phi' + \tfrac{1}{2}\tilde{u}''\phi + \kappa_0\left(\phi - \tfrac{1}{2}\tilde{u}'v'\right)\right] \tag{7}$$

$$\kappa_y = (1+\varepsilon)^{-1}\left[\tilde{u}'' - \tfrac{1}{2}v'\phi' + \tfrac{1}{2}v''\phi + \kappa_0\left(-\tfrac{1}{2}v'^2 - \tfrac{1}{2}\phi^2 + 1\right)\right] \tag{8}$$

$$\kappa_s = (1+\varepsilon)^{-1}\left[\phi' - \tfrac{1}{2}\tilde{u}'v'' + \tfrac{1}{2}\tilde{u}''v' + \kappa_0\left(v' + \tfrac{1}{2}\tilde{u}'\phi\right)\right] \tag{9}$$

where κ_0 is the initial curvature of the curved beam's centroidal locus about the Y axis, $\tilde{w}' = w' - \kappa_0 u$ and ε can be written as

$$\varepsilon \approx \tilde{w}' + \tfrac{1}{2}\tilde{u}'^2 + \tfrac{1}{2}v'^2 + \tfrac{1}{2}\tilde{w}'^2 \tag{10}$$

2.4. Strains

Using the right extensional strain definition we have

$$\mathbf{D} = \mathbf{R}\mathbf{U} - \mathbf{I} \tag{11}$$

where $\mathbf{D}$ is the deformation gradient tensor, $\mathbf{R}$ is the rotation tensor, $\mathbf{I}$ is the identity matrix and $\mathbf{U}$ is the right stretch tensor, i.e. $\mathbf{U}=\mathbf{I}+\varepsilon$. Pre-multiplying Eq. (11) by $\mathbf{R}^T$ we have

$$\mathbf{R}^T\mathbf{D} = \mathbf{I} + \boldsymbol{\varepsilon} - \mathbf{R}^T \tag{12}$$

The strain can be obtained from Eq. (12) as

$$\boldsymbol{\varepsilon} = \mathbf{R}^T\mathbf{D} - \mathbf{I} + \mathbf{R}^T \tag{13}$$

Matrix $\mathbf{D}$ is found by taking the gradient of the deformation vector with respect to x, y and s coordinates. The deformation can be defined as the difference between the initial and final position vectors $\mathbf{a}_0$ and $\mathbf{a}$.

$$\mathbf{D} = \begin{pmatrix} \frac{\partial(\mathbf{a}-\mathbf{a}_0)}{\partial x} & \frac{\partial(\mathbf{a}-\mathbf{a}_0)}{\partial y} & \frac{\partial(\mathbf{a}-\mathbf{a}_0)}{\partial s} \end{pmatrix} \tag{14}$$

Using the definitions of the position vector in Eq. (1), the deformation gradient tensor in calculated in terms of curvature components of the deformed configuration as

$$\mathbf{D} = \begin{bmatrix} 0 & 0 & (1+\varepsilon)\left(-y\kappa_s - \bar{\omega}p\kappa_y\right) \\ 0 & 0 & (1+\varepsilon)\left(x\kappa_s + \bar{\omega}p\kappa_x\right) \\ -y - \frac{\partial\bar{\omega}}{\partial x}p & x - \frac{\partial\bar{\omega}}{\partial y}p & (1+\varepsilon)\left(1 - x\kappa_y + y\kappa_x - \bar{\omega}p'\right) - \left(1 - x\kappa_0\right) \end{bmatrix} \tag{15}$$

By performing the calculations (Appendix B), the normal strain can be written as

$$\begin{aligned} \varepsilon_{ss} &= w' + \tfrac{1}{2}w'^2 + \kappa_0\left(-u - uw'\right) + \tfrac{1}{2}\kappa_0{}^2u^2 \\ &+ x\left[-u'' + \tfrac{3}{2}v'\phi' - \tfrac{1}{2}v''\phi + \kappa_0\left(-w' + \tfrac{3}{2}v'^2 + \tfrac{1}{2}\phi^2\right)\right] \\ &+ y\left[-v'' - \tfrac{3}{2}u'\phi' + \tfrac{1}{2}u''\phi + \kappa_0\left(\phi - \tfrac{3}{2}u'v' - \tfrac{3}{2}w\phi' + \tfrac{1}{2}w'\phi\right) - \tfrac{3}{2}\kappa_0{}^2v'w\right] \\ &+ \omega\left[-\phi'' + \tfrac{1}{2}u'v''' - \tfrac{1}{2}u'''v' + \kappa_0\left(-v'' - \tfrac{1}{2}u''\phi - \tfrac{1}{2}u'\phi' + \tfrac{1}{2}v'''w - \tfrac{1}{2}v'w''\right) + \tfrac{1}{2}\kappa_0{}^2\left(-w'\phi - w\phi'\right)\right] \end{aligned} \tag{16}$$

The shear strain is calculated to be

$$\gamma_{sx} = \left(-y - \frac{\partial \bar{\omega}}{\partial x} \right) (1+\varepsilon)^{-1} \left[\phi' - \tfrac{1}{2}\tilde{u}'v'' + \tfrac{1}{2}\tilde{u}''v' + \kappa_0 \left(v' + \tfrac{1}{2}\tilde{u}'\phi \right) \right] \tag{17}$$

$$\gamma_{sy} = \left(x - \frac{\partial \bar{\omega}}{\partial y} \right) (1+\varepsilon)^{-1} \left[\phi' - \tfrac{1}{2}\tilde{u}'v'' + \tfrac{1}{2}\tilde{u}''v' + \kappa_0 \left(v' + \tfrac{1}{2}\tilde{u}'\phi \right) \right] \tag{18}$$

On the other hand, from the assumption of negligible shear strain on the mid-surface, the only non-zero shear strain is through the thickness t of the plate stiffness and can be approximated as

$$\gamma_p = -2r\kappa_s = -2r(1+\varepsilon)^{-1} \left[\phi' - \tfrac{1}{2}\tilde{u}'v'' + \tfrac{1}{2}\tilde{u}''v' + \kappa_0 \left(v' + \tfrac{1}{2}\tilde{u}'\phi \right) \right] \tag{19}$$

where r is the normal distance from the mid-surface of the thin-walled element. It can be seen that Eq. (19 is compatible with Eqs. (17) and (18). Replacing $\tilde{u} = u' + \kappa_0 w$, the shear strain will be equal to

$$\gamma_p = -2r\kappa_s = -2r(1+\varepsilon)^{-1} \left[\phi' - \tfrac{1}{2}u'v'' + \tfrac{1}{2}u''v' + \kappa_0 \left(v' + \tfrac{1}{2}u'\phi - \tfrac{1}{2}v''w + \tfrac{1}{2}v'w' \right) + \tfrac{1}{2}\kappa_0{}^2 w\phi \right] \tag{20}$$

It should be noted that $2r = \sqrt{\left(-y - \frac{\partial \bar{\omega}}{\partial x} \right)^2 + \left(x - \frac{\partial \bar{\omega}}{\partial y} \right)^2}$ and $\gamma_p = \sqrt{\gamma_{sx}{}^2 + \gamma_{sy}{}^2}$ were used, and in Eq. (16) $\bar{\omega}$ is approximated as the Vlasov warping function ω (Vlasov 1961), i.e. $\omega \approx \bar{\omega}$.

2.5. Variations of strains

The first variation of the normal and shear strain can be written as

$$\delta\boldsymbol{\varepsilon} = \left\langle \delta\varepsilon_p \quad \delta\gamma_p \right\rangle^T = \mathbf{SB}\delta\boldsymbol{\theta} = \mathbf{SBN}\delta\mathbf{u} \tag{21}$$

The matrix **S** in Eq. (21) contains geometrical characteristics of the point and can be shown explicitly as

$$S = \begin{bmatrix} 1 & x & y & \omega & 0 \\ 0 & 0 & 0 & 0 & 2t_p \end{bmatrix} \tag{22}$$

The non-zero elements of matrix **B** are presented in Appendix C, and vector $\boldsymbol{\theta}$ contains displacement components of a point in the body as

$$\boldsymbol{\theta} = \langle u \;\; u' \;\; u'' \;\; u''' \;\; v \;\; v' \;\; v'' \;\; v''' \;\; w \;\; w' \;\; w'' \;\; \phi \;\; \phi' \;\; \phi'' \rangle^T \tag{23}$$

N includes shape functions that are polynomial functions of S and **u** is the nodal displacement vector (Appendix E).

3. Stresses and Stress Resultants

In this study, linear-elastic material behaviour is assumed. Correspondingly, the constitutive relations can be of the form

$$\boldsymbol{\sigma} = \left\langle \sigma_p \quad \tau_p \right\rangle^T = \begin{bmatrix} E & 0 \\ 0 & G \end{bmatrix} \begin{Bmatrix} \varepsilon_p \\ \gamma_p \end{Bmatrix} = \mathbf{E}\boldsymbol{\varepsilon} \tag{24}$$

where E and G are the Young's modulus and the shear modulus of the material, respectively. The stress resultants vector can be written as

$$\mathbf{R} = \left\langle N \quad M_x \quad M_y \quad B \quad T \right\rangle^T = \int_A \mathbf{S}^T \boldsymbol{\sigma} dA \tag{25}$$

where **N**, $\mathbf{M}_x$, **B** and T are the axial normal force, bending moments about x and y axes, bimoment and the torque, respectively, which are shown explicitly as

$$N = \int_A \sigma_p dA, \quad M_x = \int_A \sigma_p y dA, \quad M_y = \int_A \sigma_p x dA,$$

$$B = \int_A \sigma_p \omega dA, \quad T = \int_A \tau_p \left(2t_p \right) dA. \tag{26 (a-e)}$$

The cross-sectional properties associated with the above stress resultants are

$$A = \int_A dA, \quad I_{xx} = \int_A y^2 dA, \quad I_{yy} = \int_A x^2 dA,$$

$$I_{\omega\omega} = \int_A \omega^2 dA, \tag{27 (a-d)}$$

while the torsional constant associated with the torque can be written as

$$J_d \approx \tfrac{1}{3}\sum_{i=1}^{n} b_i t_i{}^3 \tag{28}$$

where n is the number of plate sections in the cross-section and b_i and t_i are the width and thickness of the i^{th} segment, respectively.

4. Loading

The vector of the external loading is defined as

$$\mathbf{Q} = \left\langle Q_x \quad Q_y \quad Q_s \quad M_{ex} \quad M_{ey} \quad M_{es} \quad B_e \right\rangle^T, \tag{29}$$

in which Q_x, Q_y and Q_s are the concentrated forces in the X, Y and S directions, respectively, M_{ex} and M_{ey} are the bending moments around X and Y axes, M_{es} is the external torque and B_e is the externally applied bimoment. The distributed external load vector can be written in the same fashion as

$$\mathbf{q} = \left\langle q_x \quad q_y \quad q_s \quad m_{ex} \quad m_{ey} \quad m_{es} \quad b_e \right\rangle^T, \tag{30}$$

The components of **q** are the counterparts of concentrated external loads of Eq. (29) distributed along the s-direction throughout the member. The concentrated and distributed loads are all applied at the centroid of the cross-section.

5. Principle of Virtual Work

5.1. Nonlinear equilibrium equations

According to the principle of virtual work, if a kinematically admissible virtual strain is applied to a structure in equilibrium, the sum of the work done by the external forces due to the virtual strain is equal to the work done internally by the stresses

$$\delta\Pi = \delta U - \delta V = 0 \tag{31}$$

where δU and δV are the variation of internal work and the variation of work done by external forces, respectively. The variation of the internal work can be written as

$$\delta U = \int_V \delta\boldsymbol{\varepsilon}^T \boldsymbol{\sigma} dV = \int_0^S \delta\mathbf{u}^T \mathbf{N}^T \mathbf{B}^T \left(\int_A \mathbf{S}^T \boldsymbol{\sigma} dA \right) ds$$

$$= \int_0^S \delta\mathbf{u}^T \mathbf{N}^T \mathbf{B}^T \mathbf{R} ds. \tag{32}$$

The virtual work done by the external loads can be written as

$$\delta V = \int_0^S \delta\mathbf{u}_q{}^T \mathbf{q} ds + \sum_{i=1}^n \delta\mathbf{u}_i{}^T \mathbf{Q}_i$$

$$= \int_0^S \delta\mathbf{u}_i{}^T \mathbf{N}_q{}^T \mathbf{A}^T \mathbf{q} ds + \sum_{i=1}^n \delta\mathbf{u}_i{}^T \mathbf{Q}_i = \delta\mathbf{u}^T \mathbf{F} \tag{33}$$

By the virtue of Eq. (31) we have

$$\delta\mathbf{u}^T \int_0^S \mathbf{N}^T \mathbf{B}^T \mathbf{R} ds = \delta\mathbf{u}^T \mathbf{F} \tag{34}$$

As the virtual displacement vector $\delta\mathbf{u}$ is arbitrary, the equilibrium equation can be written as

$$\int_0^S \mathbf{N}^T \mathbf{B}^T \mathbf{R} ds = \mathbf{F} \tag{35}$$

5.2. Consistent linearization

The incremental equilibrium equation is obtained by subtracting the expressions for virtual work at two neighbouring positions, i.e. $\delta\Pi(\mathbf{u}, \mathbf{q}, \mathbf{Q})$ and $\delta\Pi(\mathbf{u}+\delta\mathbf{u}, \mathbf{q}+\delta\mathbf{q}, \mathbf{Q}+\delta\mathbf{Q})$, and linearizing the results by omitting second and higher order terms. Using the Taylor expansion, the difference between the aforementioned virtual expressions can be approximated with the second variation of the potential as

$$\delta\Pi(\mathbf{u}+\delta\mathbf{u}, \mathbf{q}+\delta\mathbf{q}, \mathbf{Q}+\delta\mathbf{Q}) - \delta\Pi(\mathbf{u}, \mathbf{q}, \mathbf{Q}) = \Delta(\delta\Pi) \approx \delta(\delta\Pi)$$

$$= \left(\frac{\partial\delta\Pi}{\partial\mathbf{u}^T} \right) \delta\mathbf{u} + \left(\frac{\partial\delta\Pi}{\partial\mathbf{q}^T} \right) \delta\mathbf{q} + \left(\frac{\partial\delta\Pi}{\partial\mathbf{Q}^T} \right) \delta\mathbf{Q} \tag{36}$$

As matrices **B** and **R** in the equilibrium Eq. (35) are functions of the displacement vector **u**, the first term of Eq. (36) can be written as

$$\left(\frac{\partial\delta\Pi}{\partial\mathbf{u}^T} \right) \delta\mathbf{u} = \int_0^S \delta\mathbf{u}^T \mathbf{N}^T \delta\mathbf{B}^T \mathbf{R} ds + \int_0^S \delta\mathbf{u}^T \mathbf{N}^T \mathbf{B}^T \delta\mathbf{R} ds \tag{37}$$

by noting that

$$\delta\mathbf{R} = \int_A \mathbf{S}^T \mathbf{E} \delta\boldsymbol{\varepsilon} dA = \int_A \mathbf{S}^T \mathbf{E} \mathbf{S} \mathbf{B} \mathbf{N} \delta\mathbf{u} dA \tag{38}$$

Eq. (37) can be written as

$$\left(\frac{\partial\delta\Pi}{\partial\mathbf{u}^T} \right) \delta\mathbf{u} = \int_0^S \delta\mathbf{u}^T \mathbf{N}^T \delta\mathbf{B}^T \mathbf{R} ds + \delta\mathbf{u}^T \mathbf{K} \delta\mathbf{u}, \tag{39}$$

where **K** is the stiffness matrix

$$\mathbf{K} = \int_S \mathbf{N}^T \mathbf{B}^T \mathbf{D} \mathbf{B} \mathbf{N} ds \tag{40}$$

in which

$$\mathbf{D} = \int_A \mathbf{S}^T \mathbf{E} \mathbf{S} dA \tag{41}$$

is the elasticity matrix. The variation of the **B** matrix is handled by the introduction of a 14×14 matrix $\mathbf{M}_\sigma$ that satisfies the following equation

$$\delta\mathbf{B}^T \mathbf{R} = \mathbf{M}_\sigma \delta\boldsymbol{\theta} = \mathbf{M}_\sigma \mathbf{N} \delta\mathbf{u} \tag{42}$$

Consequently, Eq. (39) takes the form

$$\left(\frac{\partial\delta\Pi}{\partial\mathbf{u}^T} \right) \delta\mathbf{u} = \delta\mathbf{u}^T \int_0^S \mathbf{N}^T \mathbf{M}_\sigma \mathbf{N} \delta\mathbf{u} ds + \delta\mathbf{u}^T \mathbf{K} \delta\mathbf{u} = \delta\mathbf{u}^T \mathbf{K}_t \delta\mathbf{u} \tag{43}$$

Non-zero elements of the matrix $\mathbf{M}_\sigma$ are given explicitly

in Appendix D. The second terms of Eq. (36) can be written as

$$\left(\frac{\partial \delta \Pi}{\partial \mathbf{q}^T}\right)\delta \mathbf{q} = -\int_0^S \delta \mathbf{u}_i \mathbf{N}_q{}^T \mathbf{A}^T \delta \mathbf{q}\, ds, \tag{44}$$

and from the last term of Eq. (36),

$$\left(\frac{\partial \delta \Pi}{\partial \mathbf{Q}^T}\right)\delta \mathbf{Q} = -\sum_{i=1}^{n} \delta \mathbf{u}_i{}^T \delta \mathbf{Q}_i. \tag{45}$$

By the virtue of Eqs. (36), (43), (44) and (45), the incremental equilibrium equation can be expressed as

$$\mathbf{K}_t \delta \mathbf{u} - \delta \mathbf{F} = 0 \tag{46}$$

where $\delta\mathbf{u}$ is the incremental displacement vector and $\delta\mathbf{F}$ is the incremental load, which is shown explicitly in Eq. (47).

$$\delta \mathbf{F} = \delta \mathbf{Q} + \int_0^S \mathbf{N}_q{}^T \mathbf{A}^T \delta \mathbf{q}\, ds. \tag{47}$$

5.3. Finite element formulation

The nodal displacement vector used in the development of finite element formulation can be written as

$$\mathbf{u}_{14\times 1} = \langle w_1 \;\; w_2 \;\; u_1 \;\; u_1' \;\; u_2 \;\; u_2' \;\; v_1 \;\; v_1' \;\; v_2 \;\; v_2' \;\; \phi_1 \;\; \phi_1' \;\; \phi_2 \;\; \phi_2' \rangle^T \tag{48}$$

The displacement field functions are obtained using cubic polynomials for u, v and ϕ, and a linear interpolation function for w:

$$\begin{aligned} u(s) &= N_1 u_1 + N_2 u_1' + N_3 u_2 + N_4 u_2', \\ v(s) &= N_1 v_1 + N_2 v_1' + N_3 v_2 + N_4 v_2', \\ \phi(s) &= N_1 \phi_1 + N_2 \phi_1' + N_3 \phi_2 + N_4 \phi_2', \\ w(s) &= M_1 w_1 + M_2 w_2, \end{aligned} \tag{49}$$

N_1, N_2, N_3, and N_4 in Eq. (49) are the Hermitian polynomials

$$\begin{aligned} &N_1 = 1 - 3\xi^2 + 2\xi^3, \quad N_2 = S\left(\xi - 2\xi^2 + \xi^3\right), \\ &N_3 = 3\xi^2 - 2\xi^3, \quad N_4 = S\left(-\xi^2 + \xi^3\right) \end{aligned} \tag{50}$$

M_1 and M_2 are linear interpolations

$$M_1 = 1 - \xi, \quad M_2 = \xi, \tag{51}$$

where $\xi = s/S$ and S is the span of the member.

The nonlinear set of equilibrium equations is solved using a load-controlled Newton-Raphson incremental-iterative scheme in a step-by-step manner based on the derivations in Section 5.2. For this purpose, a residual term is introduced as

$$\Delta \mathbf{R} = \mathbf{K}_t \delta \mathbf{u} - \delta \mathbf{F} \tag{52}$$

The equilibrium conditions is deemed to be satisfied at each incremental step n at the end of k^{th} iteration if the residual is smaller than a predefined value, i.e. $\|\Delta \mathbf{R}_k^n\| < \varepsilon_{tol}$. In this study ε_{tol} is taken as 0.001% of the load increment.

It should be noted that by using a load-controlled algorithm solution, the finite element model is not capable of capturing a snap-through buckling behaviour. However, such behaviour is unlikely for horizontally-curved beams as the coupling between the bending and torsional displacement components prevents a bifurcation type of buckling (Pi & Trahair, 1997).

6. Verifications

The accuracy of the proposed model is verified in the following numerical examples by providing comparisons with results from the literature and a shell-type finite element formulation.

The plate-bending component of the shell element is developed by using Discrete Kirchhoff Quadrilateral (Batoz & Tahar, 1982) that omits the shear deformation effects to avoid shear locking in the analysis of thin plates. The finite element developed by Ibrahimbegovic *et al*. (1990) employing the drilling degree of freedom is used for the membrane component of the shell element. Using the Isoparametric formulation, a four-noded quadrilateral is developed with 6 degrees of freedom per node. The finite element is developed by adopting standard linear interpolation function for the out-of-plane displacement and Allman-type interpolation functions for the in-plane deflections. The drilling degree of freedom is interpolated using the standard bilinear functions

6.1. Simply-supported horizontally-curved beam

In the first example, simply-supported curved beams tested by Shanmugam *et al*. (1995) are analysed using the proposed beam element for verification purposes. The beams were made of hot-rolled I-section and were simply-supported spanning 5 meters, as shown in Fig. 2. The loading consisted of a vertical load applied at a distance of L_1=3.8 m from the end of the beam, and cross-sectional dimensions are depicted in Fig. 2(b).

The lateral, vertical and twist displacement were restrained at both ends (i.e. u_A=u_B=v_A=v_B=ϕ_A=ϕ_B=0) while two cases were introduced for lateral behaviour of the beam, namely "F" and "SS". The former indicates that the beam is laterally fixed (i.e. u'=ϕ'=0) while the latter denotes that only the above simply-supported boundary conditions are applied. The beams were also laterally fixed at load application point (i.e. u_C=0). The dimensions, material properties and boundary conditions of the analysed beams are shown in Table 1.

Shanmugam *et al*. (1995) also performed a finite

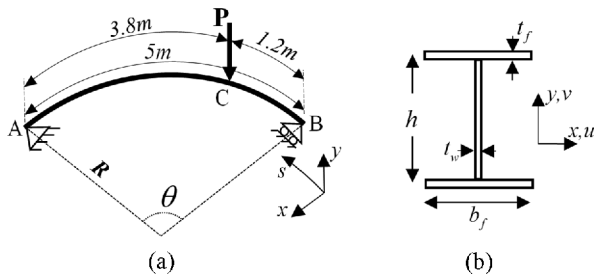

Figure 2. Cross-section, loading and boundary conditions of beams analysed in Example 1.

element modelling of the tested beam using ABAQUS (1985) curved shell elements, results of which are presented in the following figures as well. The proposed curved-beam element is used to model the behaviour of the tested curved beams using 10 beams elements. The results are then compared with the aforementioned experimental and ABAQUS results.

The vertical-displacement profile along the length of CB1 can be observed in Fig. 3 for three load levels.

It can be observed that the results of the proposed beam element formulation are in good agreement with the experimental and ABAQUS results. It should be noted that the ABAQUS results were obtained by using approximately 650 shell elements while in the current study only 10 beam elements are used. In other words, the number of degrees-of-freedom is reduced from around 4500 in the ABAQUS model to only 77 in the developed beam formulation.

The load-displacement curves for the mid-span of five CB beams can be seen in Fig. 4. Very close agreement between the rest results and the results of the proposed beam element can be confirmed. It should be noted that since the material behaviour in the developed beam element is assumed to be elastic, the elastic portion of the test results is presented herein in order to make a comparison possible.

The load-displacement at the location of the point load P is drawn in Fig. 5 for CB5. Comparing the results with the test data and ABAQUS results, the accuracy of the proposed model can be confirmed.

6.2. Cantilever curved beam

A cantilever curved beam with I-shaped cross-section is analysed in this section. The material is construction steel, which has properties of E=200 GPa, ν=0.3, and is assumed to behave elastically. The beam is subjected to vertical point load of P=1000 N applied at the tip of the

Table 1. Properties of the beams analysed in Example 1

Beam	E (GPa)	h (mm)	b_f (mm)	t_f (mm)	t_w (mm)	R (m)	θ^o	Boundary
CB1	205.1					20	14.32	F/F
CB2	210.0					30	9.55	F/F
CB3	216.2	306.6	124.3	12.1	8.0	50	5.73	SS/F
CB4	206.7					75	3.82	SS/F
CB5	206.7					150	1.91	SS/F

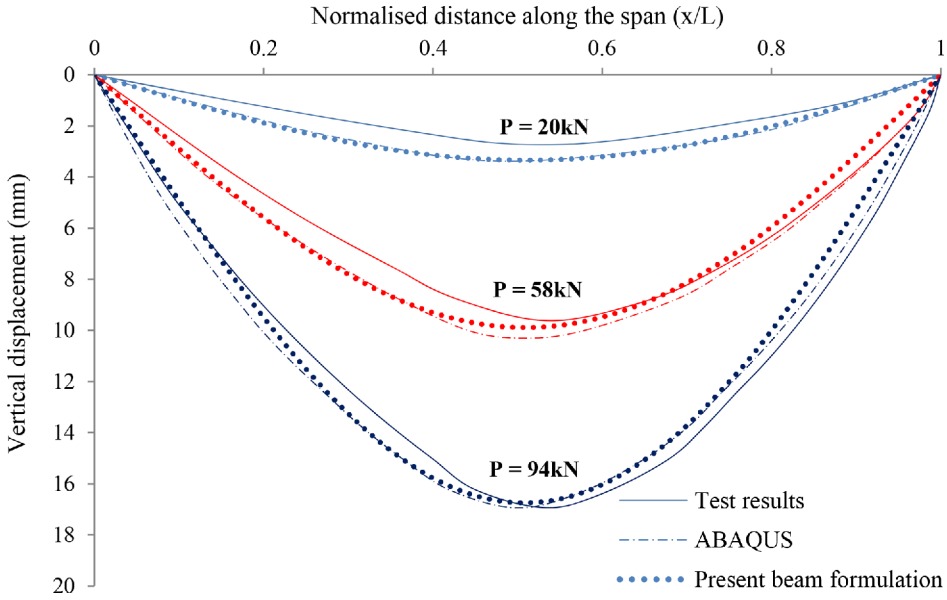

Figure 3. Displacement profile for CB1.

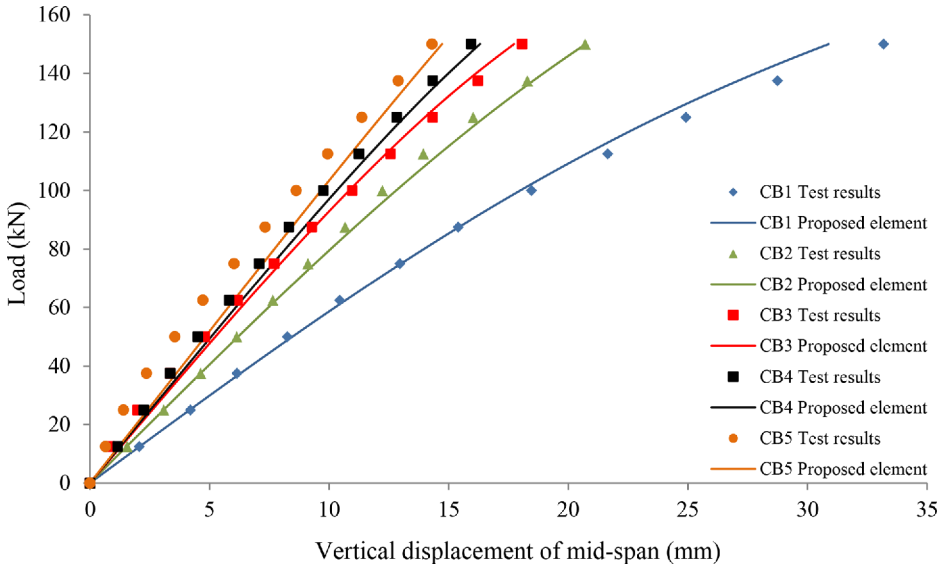

Figure 4. Load versus vertical displacement of mid-span.

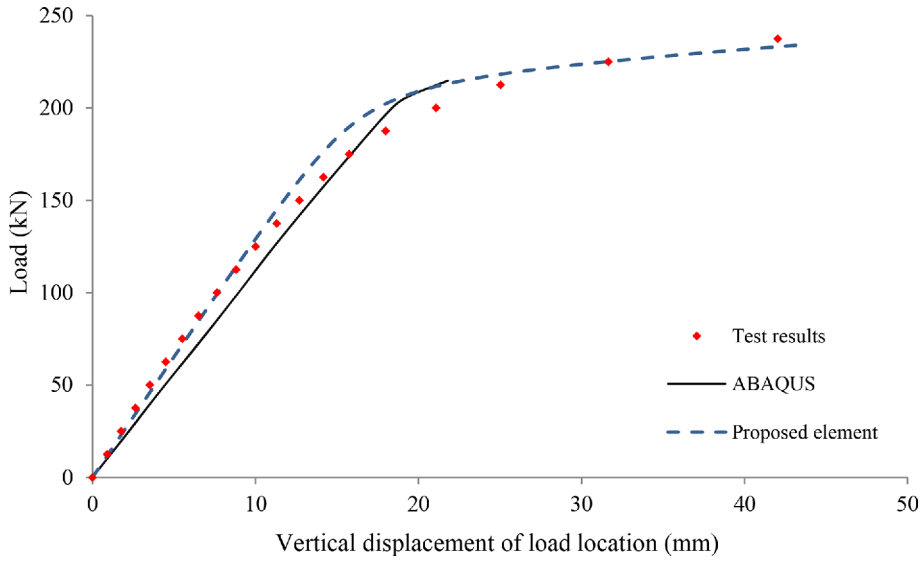

Figure 5. Load versus vertical displacement of load location for CB5.

cantilever, perpendicular to the plane of curvature. A schematic of the beam loading and boundary conditions and cross-sectional properties can be seen in Figs. 6(a) and 6(b), respectively. Cross-sectional dimensions are b_f=200 mm, h=400 mm and $t_f = t_w$=16 mm. The length of the beam is chosen as L=5000 mm.

In order to demonstrate the accuracy of the present model in the analysis of highly-curved beams, the load factor versus vertical and lateral displacements are plotted for beams with different curvature values (i.e. various included angles) using the current curved-beam formulation, results obtained from the formulation of Pi *et al*. (2005) and the shell finite element. The beam model is formed by using 10 elements of equal size while the shell model is constructed by using two shell elements for the web

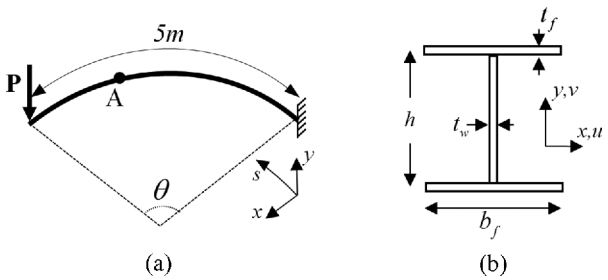

Figure 6. Schematic of cross-section, loading and boundary conditions for example 2.

and one element for each half flange, and dividing the axis of the beam into 25 pieces, which results in shell elements of 200 mm×200 mm and 100 mm×200 mm along

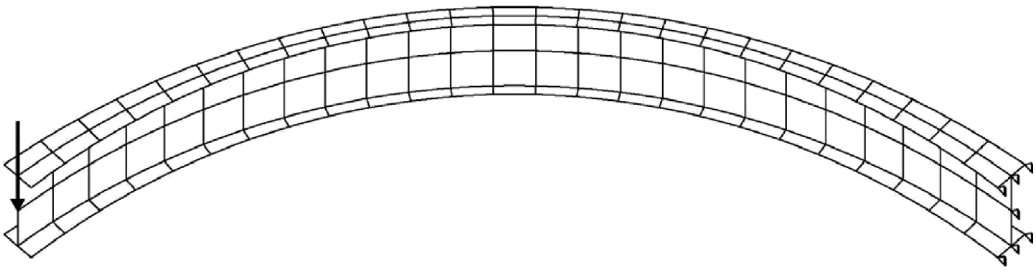

Figure 7. Shell Finite element mesh, loading and boundary conditions.

Table 2. Properties of the beams analysed in Example 2

Beam	Curvature (1/mm)	R (mm)	θ^o
B1	1.00E-05	100000	2.86
B2	1.00E-04	10000	28.65
B3	3.14E-04	3184.7	89.95

the web and flanges, respectively. All the nodes on the fixed end of the shell element are fixed in three translational directions, and the load is applied at the middle of the web of the free end of the beam (Fig. 7).

Analysis is performed for beams with 3 values of curvature, which are presented in Table 2 along with the corresponding radii and included angle values, and the displacements are plotted for point A (Fig. 6(a)) located at $3/5^{th}$ of the beam span from the support in order to exclude the local effects of point-load application in the shell analysis.

Load versus vertical displacement curves obtained from the shell finite element, curved-beam finite element of Pi *et al*. (2005) and the proposed curved-beam element are compared in Fig. 8 for 3 values of curvature and included angle. It can be observed that for small values of included angle, all the figures match. However, the results of the previous study diverges from shell results for larger values of included angle per element while the curved beam element developed herein is capable of capturing the behaviour of the beam accurately.

The lateral displacement of Point A (Fig. 6(a)) for highly curved beams B1 and B2 (Table 2) are shown in Figs. 9 and 10.

It can be observed that the current formulation is successful in capturing the nonlinear lateral displacement of the curved beam as the results are matching well with the result of the nonlinear shell finite element. It should be noted that the developed finite element formulation is shown to be capable of accurately capturing the nonlinear behaviour of highly curved beam by utilising relatively small number of element (e.g. for beam B3, the included angle per element is 8.995 degrees). It can be observed that the beam element has been able to capture the nonlinear behaviour of the beam with a significantly smaller number of degrees-of-freedom (77 instead of 1092). The total

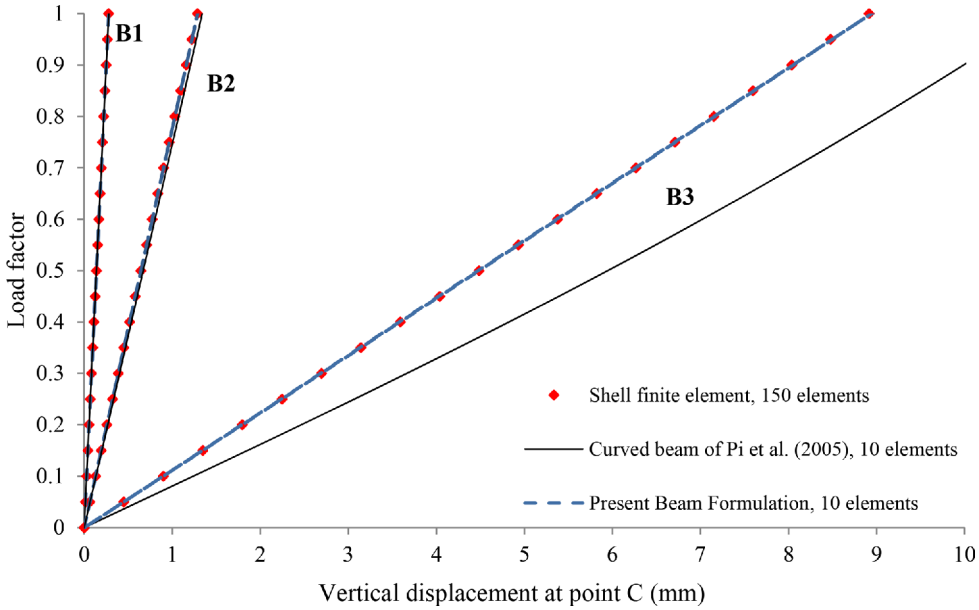

Figure 8. Load vs. vertical displacement curves for beams B1, B2 and B3.

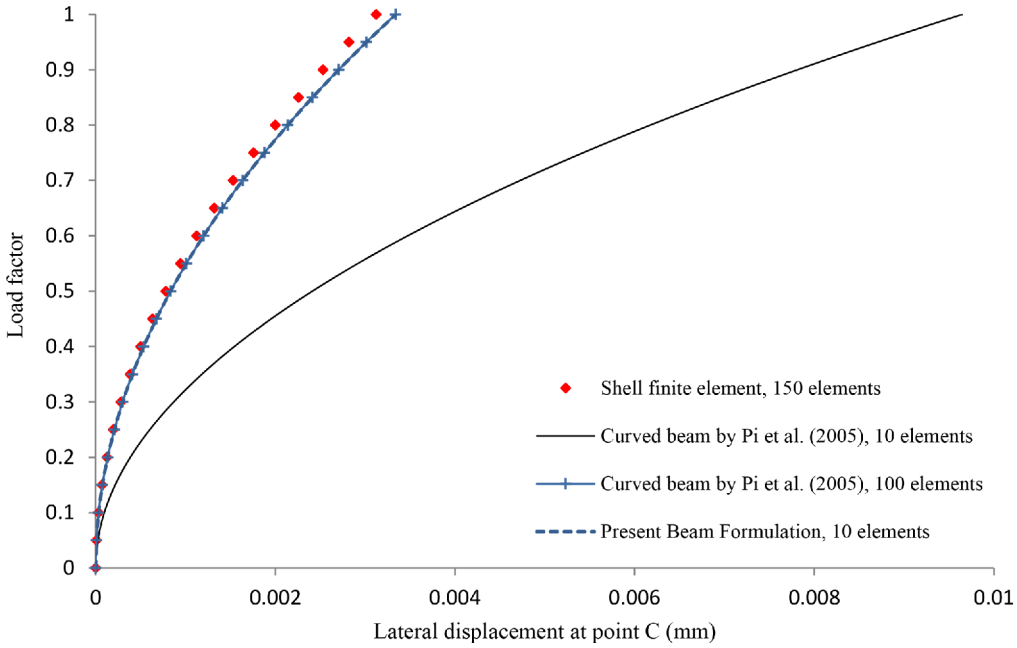

Figure 9. Load vs. lateral displacement curves for beam B2.

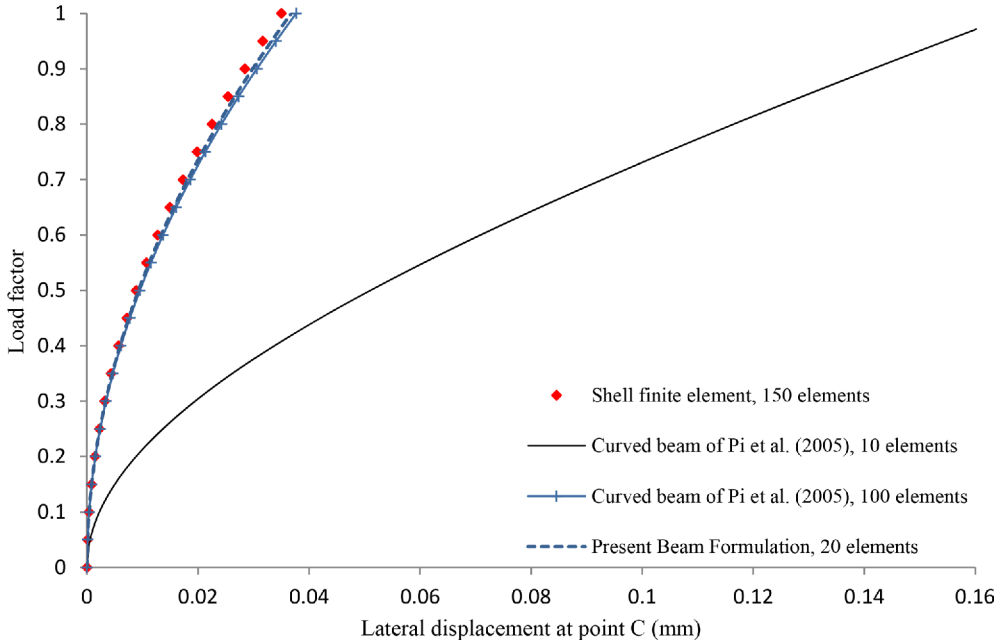

Figure 10. Load vs. lateral displacement curves for beam B3.

analysis CPU time for the beam and shell analyses are 2.283 seconds and 67.864 seconds, respectively, which is equivalent to 3.393 seconds per load increment for the shell model and 0.114 seconds per load increment for the developed element. The abovementioned CPU time values are calculated from Fortran compiler (Microsoft Visual Studio 2008) on Intel® Core i5-2400 CPU@ 3.10 GHz.

It is illustrated in Figs. 9 and 10 that the results from the curved beam formulation of Pi *et al*. (2005) converge to the result of our beam formulation when the number of elements along the beam are increased to 100.

7. Conclusions

An elastic curved-beam element is developed in this study for nonlinear analysis of thin-walled curved-in-plan members. The deformed configuration is obtained from the initial state using the Frenet-Serret formulae and a second-order rotation tensor. Right extensional strain

definition is adopted to calculate the strain terms based on the translations and rotations of the cross-section. The principle of virtual work is then used to obtain a finite element with seven degrees of freedom per node. It is assumed that the beam is curved in only one plane, and that the primary loading consists of out-of-plane loads. The results based on the developed beam formulation have been compared with experimental data and finite element results from the literature. In all cases, the accuracy of the proposed element is confirmed without necessitating the use of a large number of finite elements. It was also shown that the results of the developed formulation are very accurate for the cases where initial curvature is large.

Acknowledgments

This research was funded through a scholarship granted to the Junior Author by the Faculty of Engineering and IT at University of Technology, Sydney. Their financial support is gratefully acknowledged.

References

Akhtar, M. N. (1987). "Element stiffness of circular member", *Journal of structural engineering New York, N.Y.*, 113(4), pp. 867-872.

Basler, K. and Kollbrunner, C. F. (1969). "Torsion in structures-An engineering approach (Book on torsion emphasizing beam stressed state calculation and civil engineering problems)", *Torsion in structures-An engineering approach (Book on torsion emphasizing beam stressed state calculation and civil engineering problems)*.

Batoz, J. L. and Tahar, M. B. (1982). "Evaluation of a new quadrilateral thin plate bending element", *Int J Numer Methods Eng*, 18(11), pp. 1655-1677.

Brookhart, G. C. (1967). "Circular-arc I-type girders", *American Socienty for Civil Engineers*, vol. 93.

Crisfield, M. A. (1990). "A consistent co-rotational formulation for non-linear, three-dimensional, beam-elements", *Computer Methods in Applied Mechanics and Engineering*, 81(2), pp. 131-150.

de Veubeke, B. F. (1972). "A new variational principle for finite elastic displacements", *International Journal of Engineering Science*, 10(9), pp. 745-763.

El-Amin, F. M. and Brotton, D. M. (1976). "Horizontally curved beam finite element including warping", *International Journal for Numerical Methods in Engineering*, 10(6), pp. 1397-1406.

El-Amin, F. M. and Kasem, M. A. (1978). "Higher-order horizontally-curved beam finite element including warping for steel bridges", *International Journal for Numerical Methods in Engineering*, 12(1), pp. 159-167.

Erkmen, R. E. and Bradford, M. A. (2009). "Nonlinear elasto-dynamic analysis of I-beams curved in-plan", *International Journal of Structural Stability and Dynamics*, 9(2), pp. 213-241.

Fukumoto, Y. and Nishida, S. (1981). "Ultimate load behavior of curved I-beams", *ASCE J Eng Mech Div*, 107(2), pp. 367-385.

Ibrahimbegovic, A., Taylor, R. L., and Wilson, E. L. (1990). "Robust quadrilateral membrane finite element with drilling degrees of freedom", *International Journal for Numerical Methods in Engineering*, 30(3), pp. 445-457.

Iura, M. and Atluri, S. N. (1988). "On a consistent theory, and variational formulation of finitely stretched and rotated 3-D space-curved beams", *Computational Mechanics*, 4(2), pp. 73-88.

Koiter, W. T. (1984). "Complementary energy, neutral equilibrium and buckling", *Meccanica*, 19(1) Supplement, pp. 52-56.

Krenk, S. (1994). "A general format for curved and non-homogeneous beam elements", *Computers and Structures*, 50(4), pp. 449-454.

Love, A. E. H. (1944). *A Treatise on the Mathematical Theory of Elasticity*, 4th edn, Dover Publications Inc., New York.

Pai, P. F. and Palazotto, A. N. (1995). "Polar decomposition theory in nonlinear analyses of solids and structures", *Journal of Engineering Mechanics*, 121(4), pp. 568-581.

Pai, P. F., Palazotto, A. N., and Greer Jr, J. M. (1998). "Polar decomposition and appropriate strains and stresses for nonlinear structural analyses", *Computers and Structures*, 66(6), pp. 823-40.

Pi, Y.-L., Bradford, M. A., and Uy, B. (2005). "Nonlinear analysis of members curved in space with warping and Wagner effects", *International Journal of Solids and Structures*, 42(11-12), pp. 3147-3169.

Pi, Y. L., Bradford, M. A., and Uy, B. (2003). *Nonlinear analysis of members with open thin-walled cross-section curved in space*, University of New South Wales, School of Civil and Environmental Engineering, Sydney.

Pi, Y. L. and Trahair, N. S. (1997). "Nonlinear elastic behavior of I-beams curved in plan", *Journal of Structural Engineering*, 123(9), pp. 1201-1209.

Richard Liew, J. Y., Thevendran, V., Shanmugam, N. E., and Tan, L. O. (1995). "Behaviour and design of horizontally curved steel beams", *Journal of Constructional Steel Research*, 32(1), pp. 37-67.

Sandhu, J. S., Stevens, K. A., and Davies, G. A. O. (1990). "A 3-D, co-rotational, curved and twisted beam element", *Computers and Structures*, 35(1), pp. 69-79.

Sawko, F. (1967). "Computer analysis of grillages curved in plan", *International Association for Bridge and Structural Engineering*, vol. 8, pp. 151-170.

Shanmugam, N. E., Thevendran, V., Liew, J. Y. R., and Tan, L. O. (1995). "Experimental Study on Steel Beams Curved in Plan", *Journal of Structural Engineering*, 121(2), pp. 249-259.

Simo, J. C. (1985). "A finite strain beam formulation. The three-dimensional dynamic problem. Part I", *Computer Methods in Applied Mechanics and Engineering*, 49(1), pp. 55-70.

Simo, J. C. and Vu-Quoc, L. (1987). "The role of non-linear theories in transient dynamic analysis of flexible structures", *Journal of Sound and Vibration*, 119(3), pp. 487-508.

Simo, J. C. and Vu-Quoc, L. (1991). "A Geometrically-exact

rod model incorporating shear and torsion-warping deformation", *International Journal of Solids and Structures*, 27(3), pp. 371-393.

Vlasov, V. Z. (1961). *Thin-walled elastic beams*, 2nd edn, Israel Program for Scientific Translations, Jerusalem, Israel.

Yoo, C. H., Kang, Y. J., and Davidson, J. S. (1996). "Buckling analysis of curved beams by finite-element discretization", *Journal of Engineering Mechanics*, 122(8), pp. 762-770.

Yoshida, H. and Maegawa, K. (1983). "Ultimate strength analysis of curved I-beams", *Journal of Engineering Mechanics*, 109(1), pp. 192-214.

Young, M. C. (1969). "Flexibility influence functions for curved beams", *American Society of Civil Engineers*, vol. 94.

Appendix A

Eq. (3) can be used to obtain the deformed curvatures in terms of the initial curvature and displacement term. Differentiating Eq. (3) with respect to s yields

$$\frac{d\mathbf{q}}{ds} = \mathbf{R}\frac{d\mathbf{p}}{ds} + \frac{d\mathbf{R}}{ds}\mathbf{p} \tag{A.1}$$

where $\mathbf{q} = \begin{bmatrix} \mathbf{q}_x & \mathbf{q}_y & \mathbf{q}_s \end{bmatrix}^T$ and $\mathbf{p} = \begin{bmatrix} \mathbf{p}_x & \mathbf{p}_y & \mathbf{p}_s \end{bmatrix}^T$. We have (Pi *et al.*, 2003)

$$\frac{d\mathbf{p}}{ds} = \mathbf{K}_0\mathbf{p} \quad \frac{d\mathbf{q}}{ds^*} = \mathbf{K}\mathbf{q} \tag{A.2}$$

where $\mathbf{K}_0$ and $\mathbf{K}$ are curvature matrices in the undeformed and deformed configurations, respectively, which are defined as

$$\mathbf{K}_0 = \begin{bmatrix} 0 & 0 & -\kappa_0 \\ 0 & 0 & 0 \\ \kappa_0 & 0 & 0 \end{bmatrix} \quad \mathbf{K} = \begin{bmatrix} 0 & \kappa_s & -\kappa_y \\ -\kappa_s & 0 & \kappa_x \\ \kappa_y & -\kappa_x & 0 \end{bmatrix} \tag{A.3}$$

where κ_0 is the initial curvature of the beam and κ_x, κ_y and κ_s are the curvature values after the deformations around x, y and s axes, respectively. It should be noted that it is assumed in the formulation that the initial curvature lies in one plane only resulting in the other terms of the initial curvature matrix vanishing. ds^* in Eq. (A.2) refers to the deformed length of the beam segment, for which the relation $ds^*=(1+\varepsilon)ds$ holds, where ε is the normal strain at the centroid of the beam along the beam axis and ds is the undeformed length of the beam segment. Using the above definitions, the curvature matrix in the deformed configuration can be obtained as

$$(1+\varepsilon)\mathbf{K} = \mathbf{R}\mathbf{K}_0\mathbf{R}^T + \frac{d\mathbf{R}}{ds}\mathbf{R}^T \tag{A.4}$$

If the elements of the rotation matrix $\mathbf{R}$ are nominated as the following

$$\mathbf{R} = \begin{bmatrix} R_{11} & R_{12} & R_{13} \\ R_{21} & R_{22} & R_{23} \\ R_{31} & R_{32} & R_{33} \end{bmatrix} \tag{A.5}$$

the deformed curvature values can be obtained from the elements of the rotation matrix as

$$\kappa_x = (1+\varepsilon)^{-1}\left[\left(R_{13}R'_{12} + R_{23}R'_{22} + R_{33}R'_{32}\right) + \kappa_0\left(R_{32}R_{13} - R_{12}R_{33}\right)\right] \tag{A.6}$$

$$\kappa_y = (1+\varepsilon)^{-1}\left[\left(R_{11}R'_{13} + R_{21}R'_{23} + R_{31}R'_{33}\right) + \kappa_0\left(R_{33}R_{11} - R_{13}R_{31}\right)\right] \tag{A.7}$$

$$\kappa_s = (1+\varepsilon)^{-1}\left[\left(R_{12}R'_{11} + R_{22}R'_{21} + R_{32}R'_{31}\right) + \kappa_0\left(R_{31}R_{12} - R_{11}R_{32}\right)\right] \tag{A.8}$$

where $(\ )'$ denotes derivative with respect to s. After performing the calculations and ignoring third and higher order terms we obtain Eqs. (7)-(9) in terms of displacement components.

Appendix B

The normal strain ε_p, which is the last diagonal term in strain matrix ε, is obtained as

$$\varepsilon_{ss} = \left(\tilde{u}' - \tfrac{1}{2}\phi v'\right)(1+\varepsilon)\left(-y\kappa_s - \omega p\kappa_y\right) + \left(v' + \tfrac{1}{2}\phi\tilde{u}'\right)(1+\varepsilon)\left(x\kappa_s + \omega p\kappa_x\right) + \left[1 - \tfrac{1}{2}\left(\tilde{u}'^2 + v'^2\right)\right]\left[(1+\varepsilon)\left(1 - x\kappa_y + y\kappa_x - \omega p'\right) - \left(1 - x\kappa_0\right)\right] - 1 + \left[1 - \tfrac{1}{2}\left(\tilde{u}'^2 + v'^2\right)\right] = A + B + C + D \quad \text{(B.1)}$$

$p(s)$ is the warping amplitude function. For warping torsion it is approximated to be equal to the twist rate (Basler & Kollbrunner, 1969; Pi *et al*., 2005; Vlasov, 1961), which is the difference between the initial and final twist as

$$p(s) = \kappa_s - \kappa_{s0}, \quad \text{(B.2)}$$

and since the initial twist is assumed to be zero in this study, the warping amplitude is assumed to be equal to the final twist of the member (i.e. $p(s)=\kappa_s$). Consequently, the first term in Eq. (B.1) is calculated as

$$A = (1+\varepsilon)\left[y\kappa_s\left(-\tilde{u}' + \tfrac{1}{2}\phi v'\right) + \omega\kappa_s\kappa_y\left(-\tilde{u}' + \tfrac{1}{2}\phi v'\right)\right] = y\left[-u'\phi' + \kappa_0\left(-u'v' - w\phi'\right) - \kappa_0{}^2 v'w\right] \quad \text{(B.3)}$$

Similarly, the second term of Eq. (B.1) is equal to

$$B = (1+\varepsilon)\left[x\kappa_s\left(v' + \tfrac{1}{2}\phi\tilde{u}'\right) + \omega\kappa_s\kappa_x\left(v' + \tfrac{1}{2}\phi\tilde{u}'\right)\right] = x\left[v'\phi' + \kappa_0 v'^2\right] \quad \text{(B.4)}$$

The third term of Eq. (B.1) is re-written as

$$C = \left[1 - \tfrac{1}{2}\left(\tilde{u}'^2 + v'^2\right)\right]\left[(1+\varepsilon)\left(1 - x\kappa_y + y\kappa_x - \omega p'\right) - \left(1 - x\kappa_0\right)\right], \quad \text{(B.5)}$$

which is separated as

$$\begin{aligned} C &= \left[(1+\varepsilon)\left(1 - x\kappa_y + y\kappa_x - \omega p'\right) - \left(1 - x\kappa_0\right)\right] \\ &\quad - \tfrac{1}{2}\left(\tilde{u}'^2 + v'^2\right)\left[(1+\varepsilon)\left(1 - x\kappa_y + y\kappa_x - \omega p'\right) - \left(1 - x\kappa_0\right)\right] \\ &= E + F \end{aligned} \quad \text{(B.6)}$$

The elements of the first term of Eq. are written explicitly as the following:

$$E_1 = (1+\varepsilon) = 1 + \tilde{w}' + \tfrac{1}{2}\tilde{u}'^2 + \tfrac{1}{2}v'^2 + \tfrac{1}{2}\tilde{w}'^2 \quad \text{(B.7)}$$

$$E_2 = x(1+\varepsilon)\left(\kappa_y - \kappa_0\right) = x\left[u'' - \tfrac{1}{2}v'\phi' + \tfrac{1}{2}v''\phi + \kappa_0\left(w' - \tfrac{1}{2}v'^2 - \tfrac{1}{2}\phi^2\right)\right] \quad \text{(B.8)}$$

$$E_3 = y(1+\varepsilon)\kappa_x = y\left[-v'' - \tfrac{1}{2}u'\phi' + \tfrac{1}{2}u''\phi + \kappa_0\left(\phi - \tfrac{1}{2}u'v' - \tfrac{1}{2}w\phi' + \tfrac{1}{2}w'\phi\right) - \tfrac{1}{2}\kappa_0{}^2 v'w\right] \quad \text{(B.9)}$$

$$E_4 = \omega(1+\varepsilon)\kappa_s{}' = \omega\left[\phi'' - \tfrac{1}{2}u'v''' + \tfrac{1}{2}u'''v' + \kappa_0\left(v'' + \tfrac{1}{2}u''\phi + \tfrac{1}{2}u'\phi' - \tfrac{1}{2}v'''w + \tfrac{1}{2}v'w''\right) + \tfrac{1}{2}\kappa_0{}^2\left(w'\phi + w\phi'\right)\right] \quad \text{(B.10)}$$

The second term of Eq. (B.6) is calculated to be

$$F = -\tfrac{1}{2}\left(\tilde{u}'^2 + v'^2\right)\left[(1+\varepsilon)\left(1 - x\kappa_y + y\kappa_x - \omega p'\right) - \left(1 - x\kappa_0\right)\right] = 0 \quad \text{(B.11)}$$

It should be noted that the third and higher order terms are neglected in the above calculations. Using Eqs. (B.3) to (B.11), the normal strain can be written as

$$\begin{aligned} \varepsilon_{ss} &= w' + \tfrac{1}{2}w'^2 + \kappa_0\left(-u - uw'\right) + \tfrac{1}{2}\kappa_0{}^2 u^2 \\ &+ x\left[-u'' + \tfrac{3}{2}v'\phi' - \tfrac{1}{2}v''\phi + \kappa_0\left(-w' + \tfrac{3}{2}v'^2 + \tfrac{1}{2}\phi^2\right)\right] \\ &+ y\left[-v'' - \tfrac{3}{2}u'\phi' + \tfrac{1}{2}u''\phi + \kappa_0\left(\phi - \tfrac{3}{2}u'v' - \tfrac{3}{2}w\phi' + \tfrac{1}{2}w'\phi\right) - \tfrac{3}{2}\kappa_0{}^2 v'w\right] \\ &+ \omega\left[-\phi'' + \tfrac{1}{2}u'v''' - \tfrac{1}{2}u'''v' + \kappa_0\left(-v'' - \tfrac{1}{2}u''\phi - \tfrac{1}{2}u'\phi' + \tfrac{1}{2}v'''w - \tfrac{1}{2}v'w''\right) + \tfrac{1}{2}\kappa_0{}^2\left(-w'\phi - w\phi'\right)\right] \end{aligned} \quad \text{(B.12)}$$

Appendix C

$$
\begin{aligned}
&B_{11}=-\kappa_0-\kappa_0 w'+{\kappa_0}^2 u, && B_{1,10}=1+w'-\kappa_0 u, && B_{23}=-1,\\
&B_{26}=\tfrac{3}{2}\phi'+3\kappa_0 v', && B_{27}=-\tfrac{1}{2}\phi, && B_{2,10}=-\kappa_0,\\
&B_{2,12}=-\tfrac{1}{2}v''+\kappa_0\phi, && B_{2,13}=\tfrac{3}{2}v', && B_{32}=-\tfrac{3}{2}\phi'-\tfrac{3}{2}\kappa_0 v',\\
&B_{33}=\tfrac{1}{2}\phi, && B_{36}=-\tfrac{3}{2}\kappa_0 u'-\tfrac{3}{2}{\kappa_0}^2 w, && B_{37}=-1,\\
&B_{39}=-\tfrac{3}{2}\kappa_0\phi'-\tfrac{3}{2}{\kappa_0}^2 v', && B_{3,10}=\tfrac{1}{2}\kappa_0\phi, && B_{3,12}=\kappa_0+\tfrac{1}{2}u''+\tfrac{1}{2}\kappa_0 w',\\
&B_{3,13}=-\tfrac{3}{2}u'-\tfrac{3}{2}\kappa_0 w, && B_{42}=\tfrac{1}{2}v'''-\tfrac{1}{2}\kappa_0\phi', && B_{43}=-\tfrac{1}{2}\kappa_0\phi,\\
&B_{44}=-\tfrac{1}{2}v', && B_{46}=-\tfrac{1}{2}u'''-\tfrac{1}{2}\kappa_0 w'', && B_{47}=-\kappa_0,\\
&B_{48}=\tfrac{1}{2}u'+\tfrac{1}{2}\kappa_0 w, && B_{49}=\tfrac{1}{2}\kappa_0 v'''-\tfrac{1}{2}{\kappa_0}^2\phi', && B_{4,10}=-\tfrac{1}{2}{\kappa_0}^2\phi,\\
&B_{4,11}=-\tfrac{1}{2}\kappa_0 v', && B_{4,12}=-\tfrac{1}{2}\kappa_0 u''-\tfrac{1}{2}{\kappa_0}^2 w', && B_{4,13}=-\tfrac{1}{2}\kappa_0 u'-\tfrac{1}{2}{\kappa_0}^2 w,\\
&B_{4,14}=-1, && B_{52}=\tfrac{1}{2}v''-\tfrac{1}{2}\kappa_0\phi, && B_{53}=-\tfrac{1}{2}v',\\
&B_{56}=-\kappa_0-\tfrac{1}{2}u''-\tfrac{1}{2}\kappa_0 w', && B_{57}=\tfrac{1}{2}u'+\tfrac{1}{2}\kappa_0 w, && B_{59}=-\tfrac{1}{2}\kappa_0 v''-\tfrac{1}{2}{\kappa_0}^2\phi,\\
&B_{5,10}=-\tfrac{1}{2}\kappa_0 v', && B_{5,12}=-\tfrac{1}{2}\kappa_0 u'-\tfrac{1}{2}{\kappa_0}^2 w, && B_{5,13}=-1.
\end{aligned}
\tag{C.1}
$$

Appendix D

$$
\begin{aligned}
&M_{11}={\kappa_0}^2 R_1, && M_{1,10}=\kappa_0 R_1, && M_{26}=-\tfrac{3}{2}\kappa_0 R_3,\\
&M_{27}=\tfrac{1}{2}R_5, && M_{28}=\tfrac{1}{2}R_4, && M_{2,12}=-\tfrac{1}{2}\kappa_0 R_5,\\
&M_{2,13}=-\tfrac{3}{2}R_3-\tfrac{1}{2}\kappa_0 R_4, && M_{36}=-\tfrac{1}{2}R_5, && M_{3,12}=\tfrac{1}{2}R_3-\tfrac{1}{2}\kappa_0 R_4,\\
&M_{46}=-\tfrac{1}{2}R_4, && M_{62}=-\tfrac{3}{2}\kappa_0 R_3, && M_{63}=-\tfrac{1}{2}R_5,\\
&M_{64}=-\tfrac{1}{2}R_4, && M_{66}=3\kappa_0 R_2, && M_{69}=-\tfrac{3}{2}{\kappa_0}^2 R_3,\\
&M_{6,10}=-\tfrac{1}{2}\kappa_0 R_5, && M_{6,11}=-\tfrac{1}{2}\kappa_0 R_4, && M_{6,13}=\tfrac{3}{2}R_2,\\
&M_{72}=\tfrac{1}{2}R_5, && M_{79}=\tfrac{1}{2}\kappa_0 R_5, && M_{7,12}=-\tfrac{1}{2}R_2,\\
&M_{82}=\tfrac{1}{2}R_4, && M_{89}=\tfrac{1}{2}\kappa_0 R_4, && M_{96}=-\tfrac{3}{2}{\kappa_0}^2 R_3,\\
&M_{97}=\tfrac{1}{2}\kappa_0 R_5, && M_{98}=\tfrac{1}{2}\kappa_0 R_4, && M_{9,12}=-\tfrac{1}{2}{\kappa_0}^2 R_5,\\
&M_{9,13}=-\tfrac{3}{2}\kappa_0 R_3-\tfrac{1}{2}{\kappa_0}^2 R_4, && M_{10,1}=-\kappa_0 R_1, && M_{10,6}=-\tfrac{1}{2}\kappa_0 R_5,\\
&M_{10,10}=R_1, && M_{10,12}=\tfrac{1}{2}\kappa_0 R_3-\tfrac{1}{2}{\kappa_0}^2 R_4, && M_{11,6}=-\tfrac{1}{2}\kappa_0 R_4,\\
&M_{12,2}=-\tfrac{1}{2}\kappa_0 R_5, && M_{12,3}=\tfrac{1}{2}R_3-\tfrac{1}{2}\kappa_0 R_4, && M_{12,7}=-\tfrac{1}{2}R_2,\\
&M_{12,9}=-\tfrac{1}{2}{\kappa_0}^2 R_5, && M_{12,10}=\tfrac{1}{2}\kappa_0 R_3-\tfrac{1}{2}{\kappa_0}^2 R_4, && M_{12,12}=\kappa_0 R_2,\\
&M_{13,2}=-\tfrac{3}{2}R_3-\tfrac{1}{2}\kappa_0 R_4, && M_{13,6}=\tfrac{3}{2}R_2, && M_{13,9}=-\tfrac{3}{2}\kappa_0 R_3-\tfrac{1}{2}{\kappa_0}^2 R_4,
\end{aligned}
\tag{D.1}
$$

where

$$
\mathbf{R}=\begin{Bmatrix} R_1 & R_2 & R_3 & R_4 & R_5 \end{Bmatrix}^T \tag{D.2}
$$